

1 **Isopycnicity of cratonic mantle restricted to kimberlite provinces**

2 Artemieva<sup>1\*</sup>, I.M., Thybo, H.<sup>2,3\*</sup>, Cherepanova, Y.<sup>1,4</sup>

3 <sup>1</sup>Geology Section, IGN, University of Copenhagen, Denmark

4 <sup>2</sup>Eurasia Institute of Earth Sciences, Istanbul Technical University, Turkey

5 <sup>3</sup>Center for Earth Evolution and Dynamics (CEED), University of Oslo, Norway

6 <sup>4</sup>Wardell Armstrong International Ltd., London, UK

7 \*Corresponding authors: [thybo@geo.uio.no](mailto:thybo@geo.uio.no) and [irina@ign.ku.dk](mailto:irina@ign.ku.dk)

8  
9 **Abstract**

10 The isopycnicity hypothesis states that the lithospheric mantle of ancient platforms has a  
11 unique composition such that high density due to low lithosphere temperature is nearly  
12 compensated by low-density composition of old cratonic mantle. This hypothesis is supported  
13 by petrological studies of mantle xenoliths hosted in kimberlite magmas. However, the  
14 representativeness of the kimberlite sampling may be questioned, given that any type of  
15 magmatism is atypical for stable regions. We use EGM2008 gravity data to examine the  
16 density structure of the Siberian lithospheric mantle, which we compare with independent  
17 constraints based on free-board analysis. We find that in the Siberian craton, geochemically  
18 studied kimberlite-hosted xenoliths sample exclusively those parts of the mantle where the  
19 isopycnic condition is satisfied, while the pristine lithospheric mantle, which has not been  
20 affected by magmatism, has a significantly lower density than required by isopycnicity. This  
21 discovery allows us to conclude that our knowledge on the composition of cratonic mantle is  
22 incomplete and that it is biased by kimberlite sampling which provides a deceptive basis for  
23 the isopycnicity hypothesis.

24

25 **Highlights:**

- 26 i. Isopycnicity only applies to a small part of the Siberian craton with extensive  
27 kimberlite magmatism
- 28 ii. Kimberlites only sample anomalous, high-density lithospheric mantle
- 29 iii. The Siberian lithospheric mantle has compositional density layering
- 30 iv. The source of the Siberian LIP is likely to lie outside the craton.

31 **Keywords:** Isopycnicity, mantle density, gravity, kimberlites, lithosphere, Siberian traps

32

33 **1. Introduction: Isopycnic hypothesis - unresolved questions**

34 According to the isopycnicity hypothesis<sup>1,2</sup>, there is a trade-off between temperature  
35 and compositional density in all tectonic settings which results in almost equal density  
36 profiles everywhere. It implies for old cratons that the low density at STP (Standard  
37 Temperature and Pressure) of the lithospheric mantle is compensated by increased density by  
38 low temperature which results in relatively low topography.

39 The evolution of the cratonic lithosphere remains enigmatic. It is formed by melting  
40 of the mantle, and the product of this melting forms the lithosphere, which is lighter than the  
41 residue. and due to its positive buoyancy forms the upper layer of the Earth. Due to secular  
42 cooling of the Earth, the melting conditions in the mantle change with time<sup>3</sup>, resulting in  
43 different composition of the cratonic lithospheric mantle<sup>4</sup> produced in the early Earth by  
44 high-degree melting and at higher pressures than during the later planetary evolution<sup>5</sup>. The  
45 Archean (>2.5 Ga) lithospheric mantle is depleted in basaltic components, which makes it 2-  
46 3% lighter than younger lithospheric mantle<sup>6</sup>.

47           The Archean cratons have some of the coldest lithosphere<sup>7</sup>, which should make them  
48 heavy and gravitationally unstable. However, no geoid anomalies are associated with the  
49 cratons, which led to the isopycnicity hypothesis, whereby excess density of thermal origin of  
50 the Archean lithospheric mantle is nearly ideally compensated by density deficit due to  
51 compositional depletion<sup>1</sup>. This hypothesis, based on the mismatch between global seismic  
52 observations (with fast arrivals for seismic waves which pass the continental lithosphere in  
53 contrast to slow arrivals of waves which travel through the oceanic lithosphere) and the  
54 absence of geoid anomalies over the stable continents, has received further support from  
55 petrological studies of mantle-derived xenoliths. Based on the mineral composition of  
56 xenolith peridotites from the Kaapvaal craton in South Africa, Jordan<sup>2</sup> calculated seismic  
57 velocities and density typical of the cratonic lithospheric mantle and proposed a linear  
58 correlation between Mg# (which is a measure of mantle depletion) and mantle density. Note  
59 that this result is constrained by a geographically restricted dataset from Kaapvaal, which is  
60 further restricted to the regions of “Nature’s sampling” (kimberlite provinces).

61           The validity of the isopycnic hypothesis has been questioned since it was proposed.  
62 Three main questions are discussed, regarding (i) lateral satisfaction of isopycnicity  
63 depending on geodynamic setting, (ii) depth distribution of the density deficit in the  
64 lithospheric mantle to achieve isopycnicity, and (iii) the variation of isopycnicity with time:

65           (i) Global analysis of mantle gravity anomalies<sup>8</sup> has demonstrated that the average  
66 density of stable continental lithospheric mantle may be close to the isopycnic  
67 condition, but with significant regional deviation (with density anomalies in the  
68 lithospheric mantle with respect to the asthenosphere of up to double amplitude  
69 compared to isopycnicity predictions).

70           (ii) Assuming isopycnicity is achieved, there may be many mechanisms of density  
71 layering to bring the bulk density of the entire vertical column of the lithospheric

72 mantle to a near-isopycnic condition<sup>9</sup>, implying that at any particular depth interval  
73 isopycnicity may not be satisfied, while the entire lithospheric column may be close to  
74 isopycnic condition.

75 (iii) Given the ancient age of the cratonic lithosphere, one would expect that it may have  
76 been significantly affected by geotectonic and mantle processes. In fact, numerous  
77 petrological data from cratons worldwide provide evidence for significant  
78 metasomatic modification of the (at least, lower portions of) lithospheric mantle<sup>10-11</sup>,  
79 leading to density increase in the lower portion of the lithosphere. Recent geodynamic  
80 study of isopycnic stability over time has demonstrated that it is unlikely that this  
81 condition is stable during cratonic evolution<sup>12</sup>.

82 We use gravity data to demonstrate that isopycnicity is only fulfilled locally in cratonic  
83 regions and that petrologically studied mantle-derived xenoliths all sample cratonic  
84 lithospheric mantle where isopycnicity is satisfied. It implies that pristine lithospheric mantle,  
85 which is unsampled by Nature through xenolith-bearing kimberlite magmatism may be  
86 significantly lighter than predicted from xenolith-data and isopycnic equilibrium. To bring  
87 this highly depleted mantle to the isopycnic state, cratonic lithospheric geotherms should be  
88 significantly colder than typical xenolith P-T arrays suggest<sup>13</sup>.

## 89 2. Tectonic evolution of the Siberian craton

90 We focus on the Siberian craton (Fig. 1), since this region is covered by a high-quality  
91 regional crustal model<sup>14</sup> as required for the gravity analysis and by numerous kimberlite  
92 fields, many of which are presently studied petrologically, thus providing independent  
93 information on mantle composition<sup>15</sup>. Detailed data on the crustal structure is not available  
94 for other cratonic regions which host kimberlite provinces. This precludes similar studies for  
95 other cratons, given the importance of the crustal gravity correction for calculating mantle

96 gravity anomalies<sup>16</sup>. Even for the Kaapvaal craton, which has some of the most abundant  
97 petrological data from mantle-derived xenoliths, the existing data on the crustal structure<sup>17-19</sup>  
98 is by far insufficient for this type of high-resolution gravity study, as it is restricted to Moho  
99 depth without reliable information on seismic velocity and density structure of the crust.

100         The Siberian craton is composed of two Archean terranes, that are exposed chiefly in  
101 the Anabar shield in the north-east and the Aldan shield in the south-east, and is otherwise  
102 buried under a thick layer of sedimentary rocks ranging in age from Precambrian to  
103 Cenozoic, which is interlayered with the Siberian trap basalts in the western half of the craton  
104 (Fig. 1a). Archean blocks also outcrop at the Yenisey Ridge which marks the western edge of  
105 the craton<sup>20</sup>. The Archean terranes are separated by the Proterozoic Akitkan mobile belt  
106 which extends roughly from the Paleozoic Viluy rifted basin in the east to the southern  
107 margin of the Baikal Rift zone in the south-west towards the outcrops of the oldest dated  
108 Archean rocks in Siberia at the south-western margin of the craton. The interior parts of the  
109 craton have experienced a series of Phanerozoic tectonic and magmatic events, including the  
110 emplacement of the Siberian traps (ca. 250 Ma), several pulses of kimberlite magmatism (ca.  
111 420-380 Ma, 380-340 Ma, 245-240 Ma, and 170-140 Ma), mostly in the northern and eastern  
112 parts of the craton, and the Paleozoic large-scale Viluy rifting at the eastern terminus of the  
113 Akitkan mobile belt<sup>21</sup>.

### 114         3. Gravity analysis

115         Most of the Siberian craton is in regional isostatic equilibrium as demonstrated by  
116 near-zero (+10 to -20 mGal) free air gravity anomalies (Fig. 2a), except for isolated positive  
117 (+40+50 mGal) anomalies in the Archean shields and negative (-70-80 mGal) anomalies  
118 along the Akitkan mobile belt and the Baikal Rift zone. Bouguer gravity anomalies (Fig. 2b)

119 are between -50-150 mGal in most of the craton due to the combination of gravity effects of a  
120 relatively thick crust (Fig. 3a) and low-density upper mantle.

121 Our approach is to calculate mantle gravity anomalies as the difference between free  
122 air gravity anomalies and the gravitational effect of the crust with respect to the gravitational  
123 effect of a reference model. The reference model includes a 45 km thick crust with a density  
124 of  $2.82 \times 10^{-3} \text{ kg/m}^3$  and a 25 km thick mantle layer with density of  $3.35 \times 10^{-3} \text{ kg/m}^3$ . In this  
125 study, free air anomalies are based on EGM2008 gravity data<sup>22</sup>. However, we also performed  
126 a similar analysis<sup>16</sup> using satellite gravity data from the GOCE mission<sup>23</sup>, and the results  
127 based on the two different gravity models are consistent. The gravitational effect of the crust  
128 is computed based on the regional crustal model SibCrust<sup>14</sup> (Fig.3), which is constrained  
129 solely by seismic data and thus is suitable for gravity analysis. The SibCrust model contains  
130 information on Vp-seismic velocity and thickness of 5 crustal layers (sediments, upper,  
131 middle and lower crust, and a high velocity lower crustal layer which probably represents  
132 underplated material above Moho, where present) as well as the Pn velocity in the sub-Moho  
133 uppermost mantle (Fig. 3).

134 Gravity calculations require knowledge of the crustal density (Fig. 3b) and for each  
135 crustal layer we use a mid-curve for velocity-density conversion as reported in different  
136 laboratory studies<sup>24</sup>. For the sedimentary cover we use densities on the upper end of the  
137 corresponding Vp velocities, due to the fact that deep sedimentary basins within the Siberian  
138 craton host voluminous magmatic intrusions associated with the Siberian trap event and  
139 intracratonic rifting of the Viluy basin (Fig. 1a). The largest uncertainties in the calculation of  
140 residual mantle gravity<sup>16</sup> arise from the choice of velocity-density conversion curve (up-to  
141 0.7-1.0% for density) and the uncertainty of the thicknesses and densities of sedimentary  
142 strata (up to 0.3% for density). However, in regions with a dense network of geophysical and  
143 geological observations, the real uncertainties are significantly smaller than in synthetic tests,

144 because both the structure and composition of the sediments are constrained by observations,  
145 and physical properties of rocks are known from regional laboratory studies. Our SibCrust  
146 model is based on the wealth of data for Siberia and has high resolution of the whole crust. A  
147 dedicated analysis indicates that for the Siberian craton the uncertainty of the mantle residual  
148 anomalies may be up to ca.  $\pm 50$  mGal, as caused by uncertainty in the seismic model of the  
149 crust (thickness of crustal layers and  $V_p$  velocity in them) and uncertainty in the  $V_p$ -density  
150 conversion<sup>16</sup>. The observed mantle gravity anomalies are, however, significantly larger (with  
151 a range of ca. 400 mGal) than the maximum possible uncertainty of the gravity calculation  
152 (Fig. 4a).

#### 153 4. Mantle gravity anomalies

154 We assume that the mantle residual gravity anomalies (Fig. 4a) primarily reflect  
155 density anomalies distributed within the lithospheric mantle and integrated over the entire  
156 thickness of the chemical boundary layer above a less heterogeneous mantle below. The  
157 depth distribution of density anomalies is unknown due to inherent properties of potential  
158 fields. Gravity inversion provides information on density anomalies at in situ conditions with  
159 contributions from both compositional and thermal anomalies, which cannot be separated  
160 without additional information<sup>8</sup>. In case the isopycnic condition is satisfied, mantle gravity  
161 anomalies should be near-zero, with thermally-induced density excess being balanced by  
162 compositionally-induced density deficit.

163 The results show that, within the Siberian craton, mantle gravity anomalies range  
164 between ca. -300 mGal and ca. +50 mGal with generally negative values over the entire  
165 craton (Fig. 4a). The strongest negative residual gravity anomalies are associated with the  
166 Archean blocks which include the Anabar craton (ca. -300-250 mGal), the Yenisey Ridge (ca.  
167 -200 mGal), and the western part of the Aldan Shield (ca. -200-150 mGal) with the strongest

168 anomaly (ca. -350 mGal) in the oldest Archean block at the SW edge of the craton near the  
169 Baikal Lake. Thus the craton as a whole is not obeying isopycnicity. Negative residual mantle  
170 anomalies indicate the presence of a significant in situ density deficit within the chemical  
171 boundary layer, which is not compensated by low cratonic lithospheric temperatures. Earlier  
172 low-resolution gravity modeling<sup>8</sup> constrained by GRACE satellite data and the coarsely  
173 constrained CRUST5.0 model has indicated that the craton-average of mantle residual gravity  
174 in different Precambrian cratons may vary between ca. -90 mGal (South Africa) and ca. +70  
175 mGal (Siberia), and we attribute the difference between the two studies for Siberia to low  
176 resolution of the crustal structure in the earlier model<sup>14</sup>.

177         Near-zero mantle gravity anomalies attest to the isopycnic condition. Kimberlite  
178 magmatism, predating the Siberian traps, is only known in areas with near-zero mantle  
179 gravity, and these kimberlites are the only parts of the Siberian craton for which abundant  
180 petrological data based on mantle xenoliths exist (Fig. 4a). These kimberlites include the  
181 diamondiferous kimberlite fields of Malo-Botuoba (pipe Mir) and Daldyn-Alakit, and the  
182 kimberlite fields of the Olenek province (Fig. 1a). Near-isopycnic condition is also observed  
183 in the western part of the craton which is covered by the Siberian traps. Within kimberlite  
184 provinces, notable deviations from isopycnicity are only in regions with young (mostly 140-  
185 170 Ma) kimberlites, such as along the eastern slope of the Anabar Shield, where mantle  
186 gravity anomalies are negative. However, for the kimberlites around the Anabar Shield  
187 (except for the Kharamai field)<sup>25</sup>, geochemical studies are limited to the emplacement age and  
188 do not provide information on the composition and thereby on density of the lithospheric  
189 mantle.

190         We conclude that all petrologically studied kimberlite-hosted xenoliths sample  
191 anomalous mantle of the Siberian Craton that exhibits isopycnic behavior. On the whole,  
192 only much less than half of the Siberian Craton shows mantle gravity anomalies around zero,



193 corresponding to isopycnicity equilibrium, whereas the major part of the craton (where  
194 geochemical data on mantle composition is absent) shows large deviations from zero mantle  
195 gravity anomaly. In particular, the pristine Archean mantle in the Aldan and Anabar shields  
196 and in the Archean blocks along the western margin of the Siberian craton has a significantly  
197 smaller mantle density than isopycnicity predicts. Similarly, major parts of the central and  
198 western Siberian Craton show low mantle gravity anomalies of ca. -100 mGal or lower.

199         Our results for the Siberian craton are similar to recent results for the cratons of  
200 southern Africa<sup>26,27</sup>, where the isopycnicity condition is also satisfied only locally and mostly  
201 in the kimberlite provinces of the northwestern Kaapvaal craton, with the largest deviations in  
202 the Limpopo belt where the density of the lithospheric mantle is higher than in the Kaapvaal.  
203 Similar to the Siberian craton, the lithospheric mantle with the lowest density lies outside of  
204 the south African kimberlite clusters.

205         Our results support early observations of uncharacteristic sampling of the cratonic  
206 lithosphere mantle by mantle-derived xenoliths based on the spatial correlations between  
207 xenolith locations and in situ anomalies in upper mantle seismic velocities<sup>28</sup>. Furthermore,  
208 seismic velocity anomalies corrected for lateral temperature variations also have reduced  
209 amplitude in cratonic regions affected by kimberlite magmatism as compared to strong  
210 positive  $V_s$  velocity anomalies of non-thermal origin typical of the “intact” cratonic mantle<sup>29</sup>,  
211 which have been interpreted as the evidence that kimberlite-hosted xenoliths provide biased  
212 sampling of cratonic mantle.

## 213         5. Discussion

214         We test our results by an independent approach which is based on free-board  
215 constraints<sup>30</sup> and overlaps with our gravity calculations only in the use of the same crustal  
216 density model. Free-board calculations are based on the assumption of regional isostatic

217 equilibrium, which is justified by near-zero free air gravity anomalies (Fig. 2a). The approach  
218 is based on Archimedes' principle and assumes that surface topography originates from  
219 buoyancy of the crust and the lithospheric mantle which depend on thickness and average  
220 density of the corresponding layers. As crustal thickness and density, as well as lithosphere  
221 thickness and temperature are constrained, one can calculate regional variations in density of  
222 the lithospheric mantle at in situ and room P-T conditions from the topography. We limit the  
223 comparison of gravity and free-board calculations to in situ conditions, given that mantle  
224 gravity anomalies (Fig. 4a) and the isopycnicity condition both refer to in situ pressures and  
225 temperatures.

226         The results show geographical correlation between mantle gravity anomalies and  
227 mantle density anomalies when density anomalies are assumed to be distributed within the  
228 layer from the Moho down to the lithosphere base<sup>31</sup> (the latter is constrained by heat flow and  
229 xenolith geotherms<sup>7</sup>). However, the results of the gravity and free-board analysis are in a  
230 striking agreement (Fig. 4a,b) when assuming a layered structure of the lithospheric mantle,  
231 where the density anomalies reside mainly in an upper depleted layer between the Moho and  
232 a depth of 180 km above a fertile lower layer extending from 180 km depth down to the  
233 lithosphere base. This assumption of a layered compositional structure of the lithospheric  
234 mantle is supported by xenolith data from the Slave and the Karelian cratons<sup>31,32</sup>, and may be  
235 a common feature of cratonic lithosphere as demonstrated by some geophysical studies<sup>29</sup>.  
236 Regional xenolith studies from the Siberian craton also indicate a strong metasomatic  
237 signature in the lower part of the Siberian lithospheric mantle<sup>10</sup>, with a sharp increase of the  
238 portion of melt-metasomatised peridotites in the Archean Siberian mantle below a depth of  
239 ca. 150-180 km<sup>33</sup>.

240         In accord with petrological studies, we interpret the increased density of the  
241 lithospheric mantle in kimberlite provinces of the Siberian craton (as compared to regions

242 unaffected by the Devonian kimberlite magmatic event) by regional-scale melt-  
243 metasomatism associated with voluminous intrusions of basaltic magmas into depleted  
244 cratonic lithosphere<sup>11, 28, 31, 34</sup> (Fig. 5). Such magmatism is associated with introduction of  
245 iron-rich melts which have high density (thus positive residual gravity anomalies) and low  
246 seismic (in particular,  $V_s$ ) velocity<sup>6, 35</sup>. The role of other mineral phases (such as a decrease in  
247 orthopyroxene content during metasomatism and changes in the content of garnet and  
248 clinopyroxene) on bulk physical properties of lithospheric mantle may also be important; but  
249 there is insufficient laboratory data on bulk density of peridotite mantle as a function of  
250 orthopyroxene content<sup>36</sup> to assess their roles.

251 We observe negative mantle gravity anomalies in the north-western part of the Siberian  
252 craton, which is covered by the Siberian traps and presumably was affected by the Siberian  
253 LIP<sup>11</sup>. Such anomalies are typical of most of the Siberian craton north of the Akitkan belt,  
254 where geochemical data from abundant kimberlite-hosted xenoliths indicate the presence of  
255 depleted and moderately metasomatised cratonic mantle<sup>10</sup>. We speculate that large-scale  
256 magmatism associated with the Siberian LIP would have produced a significant metasomatic  
257 reworking of the cratonic mantle, which we do not observe in mantle gravity anomalies. Our  
258 results provide support for a thermomechanical model<sup>37</sup> of the Siberian LIP province, where  
259 the impact of a mantle hotspot was assumed to be along the north-western margin of the  
260 craton. Our observation therefore indicates that the source of the Siberian LIP is likely to lie  
261 outside the craton.

## 262 6. Conclusion

263 Our results show that:

- 264 (i) the Siberian lithospheric mantle is highly heterogeneous as evidenced by large regional  
265 variations in in situ density,

- 266 (ii) xenolith evidence on isopycnicity is restricted to cratonic mantle which may have been  
267 reworked by voluminous magmatism and where gravity calculations also indicate  
268 isopycnicity;
- 269 (iii) the Siberian lithospheric mantle is likely to have compositional (density) layering with a  
270 marked transition at a depth of 160-80 km;
- 271 (iv) the source of the Siberian LIP is likely to lie outside the craton.

272 The fact that xenolith-analysed magmatism is only observed in regions that are in  
273 isopycnicity equilibrium, indicates that this is a transient condition which is not inherent to  
274 the pristine Archean mantle. A direct consequence of this conclusion is that our knowledge  
275 on the composition of the cratonic mantle is biased by Nature's sampling. As a result, the  
276 composition of the pristine cratonic mantle remains unknown and laboratory studies of  
277 densities and seismic velocities of mantle-derived peridotites from kimberlite provinces  
278 cannot be used for meaningful interpretation of the general composition of the pristine mantle  
279 from seismic and gravity data. Furthermore, lack of information on the composition of the  
280 most pristine parts of the Archean lithospheric mantle hampers our understanding on the  
281 mechanisms of lithosphere formation in the Archean<sup>38</sup> and the mechanisms of long-term  
282 preservation of cratonic lithospheric keels<sup>39</sup>.

283

284 **References**

- 285 1. T. H. Jordan, Composition and development of the continental tectosphere, *Nature* **274**,  
286 544–548 (1978).
- 287 2. T. H. Jordan, Continents as a chemical boundary layer, *Phil. Trans. Roy. Soc. London A*  
288 **301**, 359–373 (1981).
- 289 3. C. Herzberg, K. Condie, J. Korenaga, Formation of cratonic lithosphere: An integrated  
290 thermal and petrological model, *Earth Planet. Sci. Lett.* **292**, 79–88 (2010).
- 291 4. O. F. Gaul, W. L. Griffin, S. Y. O'Reilly, N. J. Pearson, Mapping olivine composition in  
292 the lithospheric mantle, *Earth Planet. Sci. Lett.* **182**, 223–235 (2000).
- 293 5. M. J. Walter, Melting of garnet peridotite and the origin of komatiite and depleted  
294 lithosphere, *J. Petrol.* **39**, 29–60 (1998).
- 295 6. R. W. Carlson, G. Pearson, D. E. James, Physical, chemical, and chronological  
296 characteristics of continental mantle, *Rev. Geophys.* **43**, RG1001 (2005).
- 297 7. I. M. Artemieva, Global  $1^\circ \times 1^\circ$  thermal model TC1 for the continental lithosphere:  
298 Implications for lithosphere secular evolution, *Tectonophysics* **416**, 245–277 (2006).
- 299 8. M. K. Kaban, P. Schwintzer, I. M. Artemieva, W. D. Mooney, Density of the  
300 continental roots: compositional and thermal effects, *Earth Planet. Sci. Lett.* **209**, 53–69  
301 (2003).
- 302 9. R. K. Kelly, P. B. Kelemen, M. Jull, Buoyancy of the continental upper mantle,  
303 *Geochem. Geophys. Geosyst.* **4(2)**, 1017 (2003).
- 304 10. A. M. Agashev, D. A. Ionov, N. P. Pokhilenko et al., Metasomatism in lithospheric  
305 mantle roots: Constraints from whole-rock and mineral chemical composition of  
306 deformed peridotite xenoliths from kimberlite pipe Udachnaya, *Lithos* **160**, 201–215  
307 (2013).

- 308 11. G. H. Howarth, P. H. Barry, J. F. Pernet-Fisher et al., Superplume metasomatism:  
309 Evidence from Siberian mantle xenoliths, *Lithos* **184**, 209-224 (2014).
- 310 12. D. W. Eaton, H. K. C. Perry, Ephemeral isopycnicity of cratonic mantle keels, *Nature*  
311 *Geoscience* **6**, 967-970 (2013).
- 312 13. L. R. Rudnick, A. A. Nyblade, The thickness and heat production of Archean lithosphere:  
313 Constraints from xenolith thermobarometry and surface heat flow, in *Mantle Petrology:*  
314 *Field Observations and High Pressure Experimentation: A Tribute to Francis R. (Joe)*  
315 *Boyd*, Y. Fei, C. M. Bertka, B. O. Mysen, Eds. (Chem. Soc. Spec. Publ., 1999), No. 6, 3–12.
- 316 14. Y. Cherepanova, I. M. Artemieva, H. Thybo, Z. Chemia, Crustal structure of the Siberian  
317 craton and the West Siberian basin: An appraisal of existing seismic data,  
318 *Tectonophysics* **609**, 154-183 (2013).
- 319 15. H. Thybo, I. Artemieva, B. Kennett (eds.), Moho: 100 years after Andrija Mohorovičić,  
320 *Tectonophysics* **609**, 734 pp. (2013).
- 321 16. M. Herceg, I. M. Artemieva, H. Thybo, Sensitivity analysis of crustal correction for  
322 calculation of lithospheric mantle density from gravity data, *Geophys. J. Int.*, doi  
323 10.1093/gji/ggv431 (2015).
- 324 17. M. Youssof, H. Thybo, I. M. Artemieva, Moho depth and crustal composition in  
325 southern Africa, *Tectonophysics* **609**, 267-287 (2013).
- 326 18. S. K. Nair, S. S. Gao, K. H. Liu, P. G. Silver, Southern African crustal evolution and  
327 composition: constraints from receiver function studies, *J. Geophys. Res.* **111**, B02304  
328 (2006).
- 329 19. E. M. Kgaswane, A. A. Nyblade, J. Julia, et al., Shear wave velocity structure of the  
330 lower crust in southern Africa: evidence for compositional heterogeneity within  
331 Archaean and Proterozoic terrains, *J. Geophys. Res.* **114**, B12304 (2009).

- 332 20. D. Gladkochub, S. A., Pisarevsky, T. Donskaya, et al., Siberian Craton and its evolution  
333 in terms of Rodinia hypothesis, *Episodes* **29**, 169-174 (2006).
- 334 21. O. M. Rosen, K. Condie, L. M. Natapov, A. D. Nozhkin, Archean and early Proterozoic  
335 evolution of the Siberian Craton: a preliminary assessment, in *Archean Crustal*  
336 *Evolution*, K. Condie, Ed. (Elsevier, 1994), 411–459.
- 337 22. N. K. Pavlis, S. A. Holmes, S. C. Kenyon, J. K. Factor, The development and  
338 evaluation of the Earth Gravitational Model 2008 (EGM2008), *J. Geophys. Res.* **117**,  
339 B04406 (2012).
- 340 23. R. Pail, S. Bruinsma, F. Migliaccio, et al., First GOCE gravity field models derived by  
341 three different approaches, *J. Geodesy* **85**, 819-843 (2011).
- 342 24. N. I. Christensen, W. D. Mooney, Seismic velocity structure and composition of the  
343 continental crust: a global view, *J. Geophys. Res. Solid Earth* **100**, 9761–9788 (1995).
- 344 25. W. L. Griffin, L. M. Natapov, S.Y. O'Reilly, et al., The Kharamai kimberlite field,  
345 Siberia: Modification of the lithospheric mantle by the Siberian Trap event, *Lithos* **81**,  
346 167–187 (2005).
- 347 26. I.M. Artemieva, L.P. Vinnik, Density structure of the cratonic mantle in Southern Africa:  
348 1. Implications for dynamic topography, *Gondwana Research* **39**, 204–216 (2016).
- 349 27. I.M. Artemieva, L.P. Vinnik, Density structure of the cratonic mantle in Southern Africa:  
350 2. Correlations with kimberlite distribution, seismic velocities, and Moho sharpness,  
351 *Gondwana Research* **36**, 14–27 (2016).
- 352 28. W. L. Griffin, S. Y. O'Reilly, J. C. Afonso, G. C. Begg, The composition and evolution  
353 of lithospheric mantle: a re-evaluation and its tectonic implications, *J. Petrol.* **50**, 1185-  
354 1204 (2009).
- 355 29. I. M. Artemieva, The continental lithosphere: reconciling thermal, seismic, and  
356 petrologic data, *Lithos* **109**, 23-46 (2009).

- 357 30. Y. Cherepanova, I. M. Artemieva, Density heterogeneity of the cratonic lithosphere: A  
358 case study of the Siberian craton, *Gondwana Research* **28**, 1344–1360 (2015).
- 359 31. S. Aulbach, W. Griffin, N. Pearson, et al., Nature and timing of metasomatism in the  
360 stratified mantle lithosphere beneath the central Slave craton (Canada), *Chem. Geology*  
361 **352**, 153-169 (2013).
- 362 32. M. Lehtonen, H. E. O'Brien, P. Peltonen, B. S. Johanson, L. Pakkanen, Layered mantle  
363 at the Karelian Craton margin: P-T of mantle xenocrysts and xenoliths from the Kaavi–  
364 Kuopio kimberlites, Finland, *Lithos* **77**, 593–608 (2004).
- 365 33. W.L. Griffin, S.Y. O'Reilly, N. Abe, et al., The origin and evolution of Archean  
366 lithospheric mantle, *Precamb. Res.* **127**, 19-41 (2003).
- 367 34. J. E. Nielson, H. G. Wilshire, Magma transport and metasomatism in the mantle: A  
368 critical review of current geochemical models, *Am. Mineralogist* **78**, 1117-1134  
369 (1993).
- 370 35. C.-T. A. Lee, Compositional variation of density and seismic velocities in natural  
371 peridotites at STP conditions: Implications for seismic imaging of compositional  
372 heterogeneities in the upper mantle, *J. Geophys. Res. Solid Earth* **108**, 2441 (2003).
- 373 36. M. G. Kopylova, J. Lo, N. I. Christensen, Petrological constraints on seismic properties  
374 of the Slave upper mantle (Northern Canada), *Lithos* **77**, 493–510 (2004).
- 375 37. S. V. Sobolev, A. V. Sobolev, D. V. Kuzmin, et al., Linking mantle plumes, large  
376 igneous provinces and environmental catastrophes, *Nature* **477**, 312-316 (2011).
- 377 38. C.-T. A. Lee, Geochemical/petrologic constraints on the origin of cratonic mantle, in  
378 *Archean Geodynamics and Environments*, K. Benn, J.-C. Mareschal, K. C. Condie, Eds.  
379 (AGU Geophys. Monogr. (2006), v. 164.



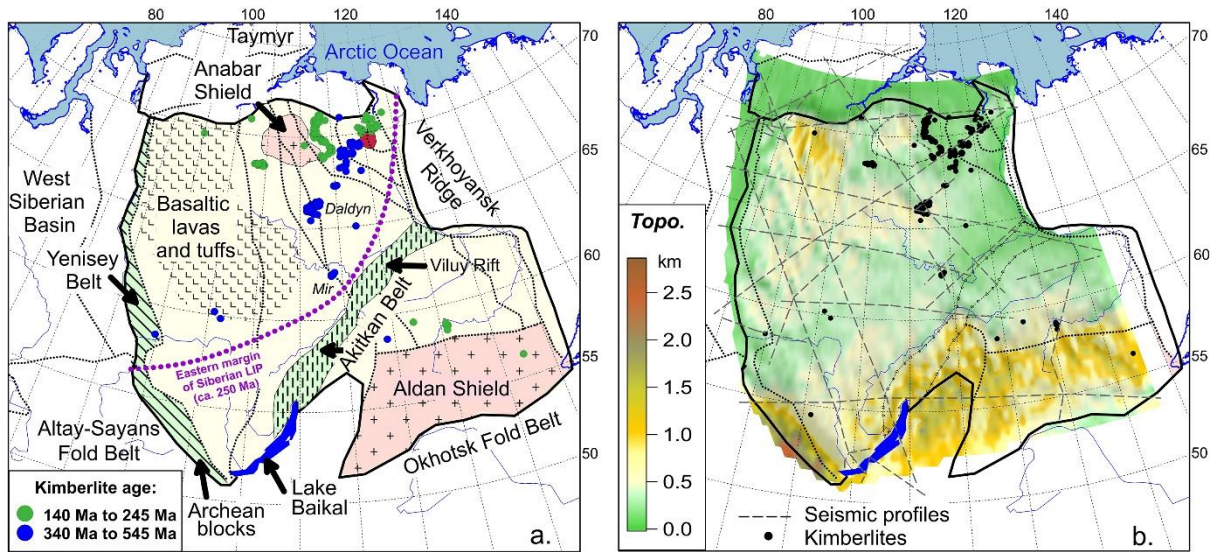
380 39. A. Lenardic, L. N. Moresi, H. Muhlhaus, Longevity and stability of cratonic lithosphere:  
381 Insights from numerical simulations of coupled mantle convection and continental  
382 tectonics, *J. Geophys. Res. Solid Earth* **108**, B6, 2303 (2003).

383

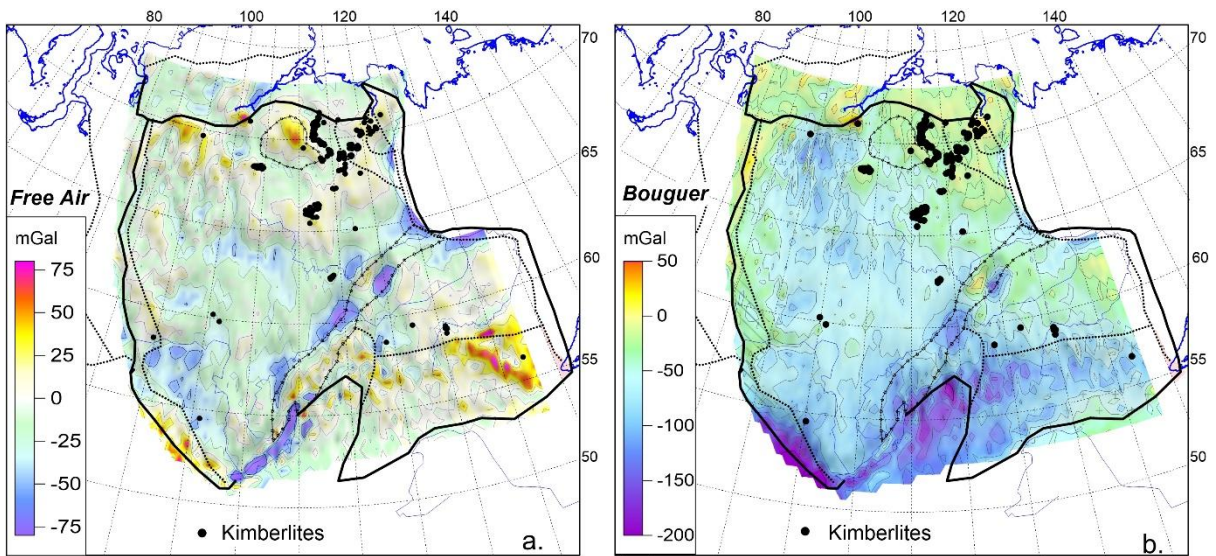
384

385 **Acknowledgments:** IA acknowledges DFF (Independent Research Fund Denmark) grant  
386 FNU-1323-00053, and HT acknowledges DFF grant FNU-16/059776-15.

387

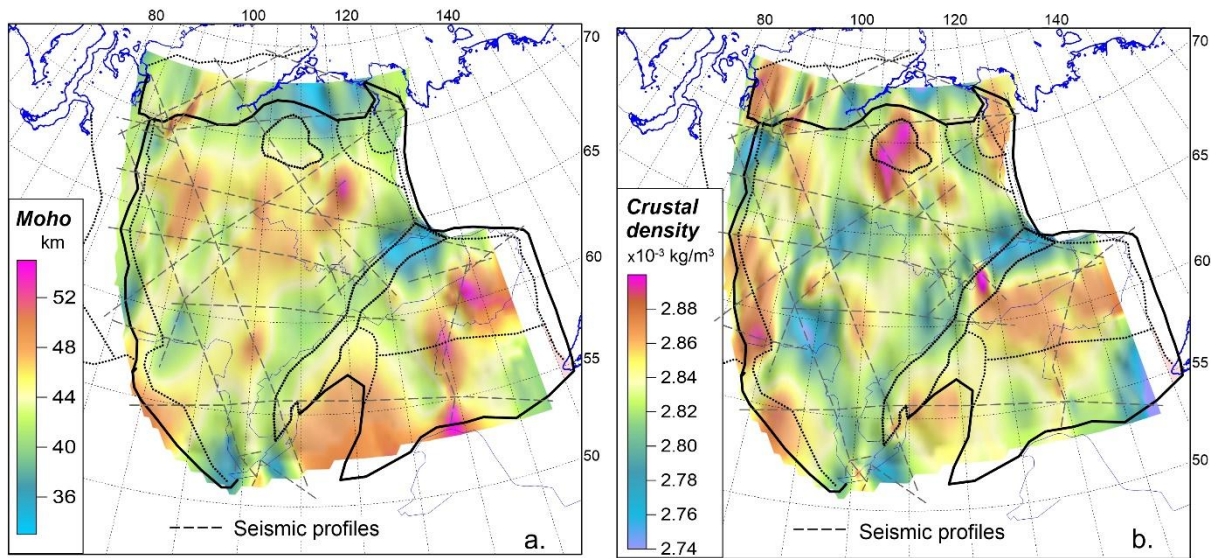


388 **Fig. 1. (a)** Simplified geological map of the Siberian craton (after ref. 21). Pink colors –  
 389 Archean shields; dark red – the Olenek Uplift; solid black line – outline of the craton; dotted  
 390 black lines – boundaries between major cratonic terranes; dotted purple line – margin of the  
 391 Siberian LIP (after ref. 11). Color dots – kimberlites (blue – erupted prior to the Siberian  
 392 traps, green – post-trap). **(b)** Topographic map with the location of major crustal-scale  
 393 seismic profiles superimposed by dashed lines used in the SibCrust regional crustal model  
 394 (ref. 14).  
 395



397 **Fig. 2.** Free air (a) and Bouguer (b) gravity anomalies based on EGM2008 gravity data (*ref.*  
398 22). Dotted lines – major tectonic boundaries; symbols – kimberlites.

400



401

402

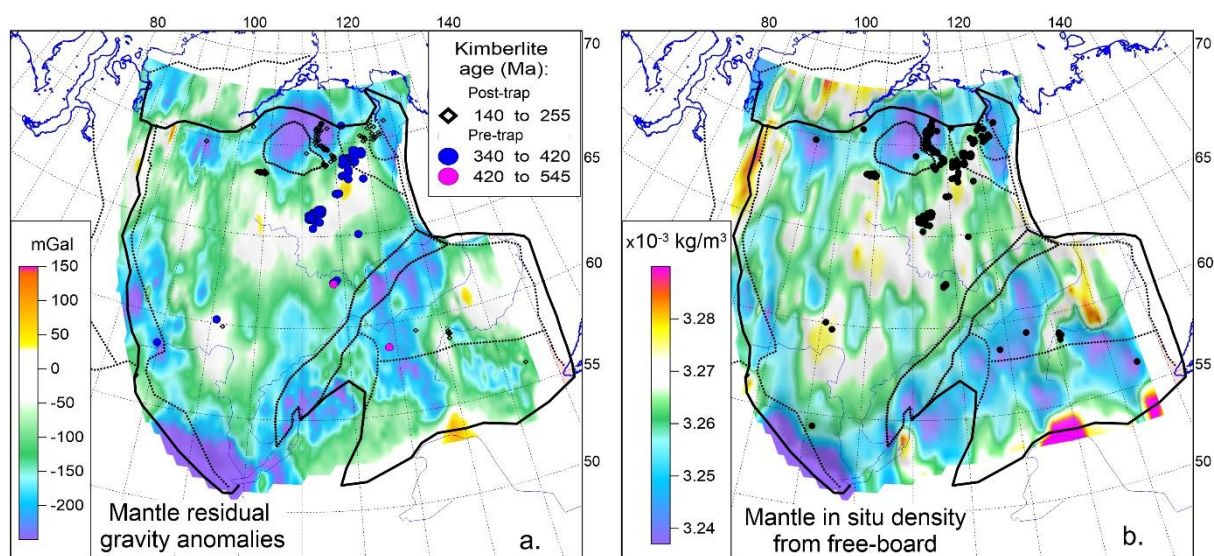
403 **Fig. 3.** Crustal structure of the Siberian craton (based on ref. 14): **(a)** Moho depth , **(b)**

404 average crustal density (including sediments). Dotted lines – major tectonic boundaries;

405 dashed lines - crustal-scale seismic profiles.

406

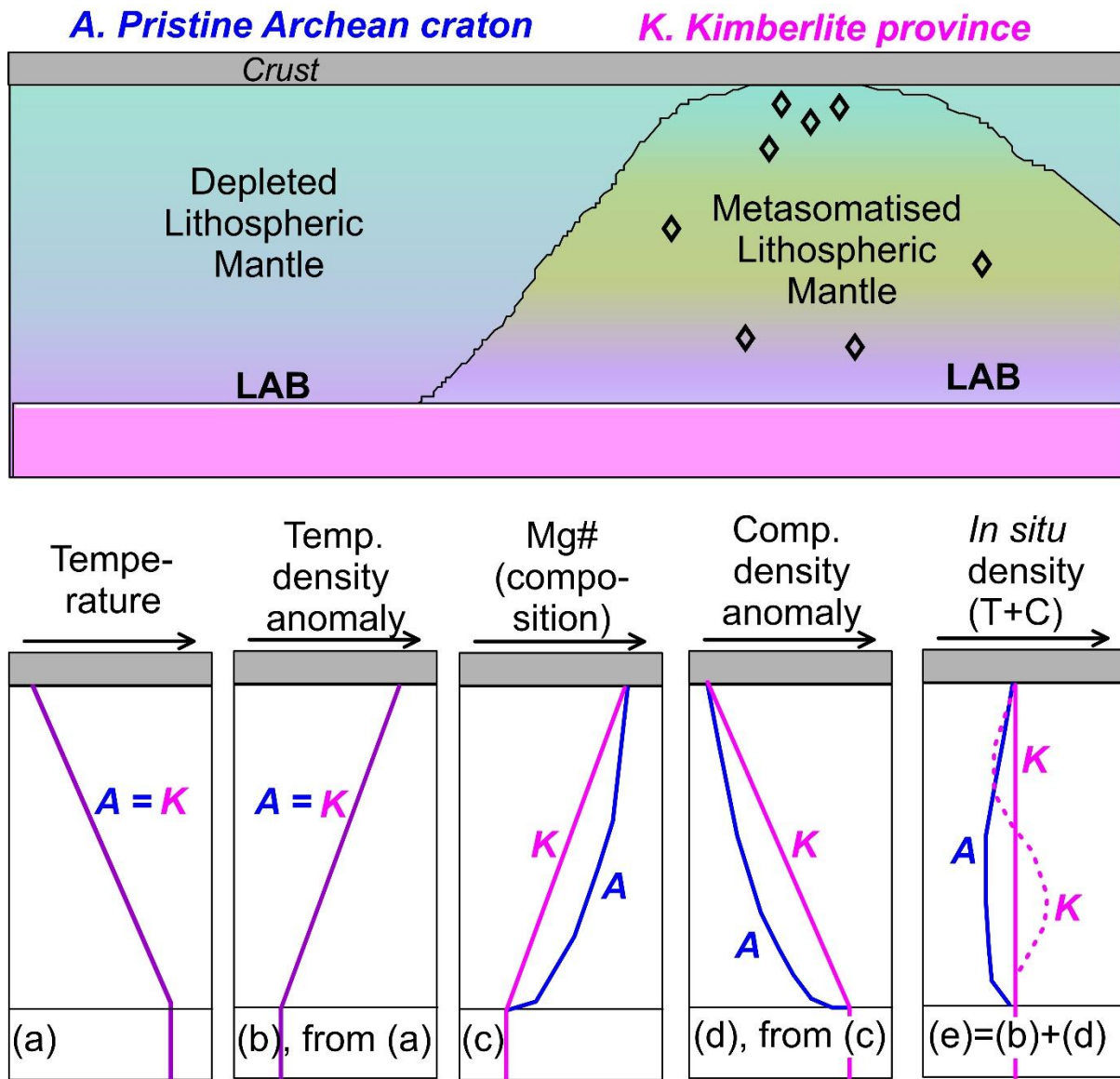




407

408 **Fig. 4.** (a) Mantle residual gravity anomalies calculated from EGM2008 gravity data. The  
 409 anomalies reflect density heterogeneity of lithospheric mantle beneath the Siberian craton. In  
 410 case the isopycnic condition is satisfied, thermally-induced density excess is balanced by  
 411 compositionally-induced density deficit, and residual mantle gravity anomalies are near-zero.  
 412 Isopycnicity is satisfied in white areas; the uncertainty of gravity anomalies is not larger than  
 413  $\pm 50$  mGal (ref. 16). (b) In situ mantle density anomalies based on free-board modeling (after  
 414 ref. 28). The anomalies are assumed to be restricted to the layer between the Moho and 180  
 415 km depth. The lithospheric mantle below 180 km and down to the lithosphere base is  
 416 assumed to have constant density of  $3.38 \text{ g/cm}^3$  (at room P-T conditions). Density of  
 417 sublithospheric mantle at room P-T conditions is assumed to be  $3.39 \text{ g/cm}^3$ . The strong  
 418 agreement between the gravity (a) and density (b) models of lithospheric mantle suggests that  
 419 layered structure of cratonic lithosphere may be a common phenomenon. Dotted lines –  
 420 major tectonic boundaries; symbols – kimberlites (color-coded by eruption age in (a)).

421



422

423 **Fig. 5.** Sketch of the principle of isopycnicity<sup>1,2</sup>. Upper panel: schematic model of a pristine

424 Archean mantle lithosphere (A) and a metasomatised mantle lithosphere typical of

425 kimberlite provinces (K). Both regions have the same thickness of the thermal boundary

426 layer, i.e. the same depth to the Lithosphere-Asthenosphere Boundary (LAB). Lower panel:

427 The five diagrams show schematic depth profiles for the following parameters: (a)

428 temperature and (b) density anomaly caused by temperature (these lines overlap for profiles

429 A and K because they have the same LAB depth); (c) Mg# where the pristine Archean

430 lithosphere is highly depleted in basaltic components and has higher Mg# values than the

431 metasomatised lithosphere; (d) compositional density anomaly caused by variation in Mg#;

432 and (e) in situ density from combining (b) and (d). The constant in situ density depth profile  
433 in the metasomatised mantle shows perfect isopycnicity (isopycnicity in its strong form, solid  
434 line). Alternatively (and probably more likely), isopycnicity may be satisfied not at every  
435 depth but when averaged over the entire vertical column of the lithospheric mantle  
436 (isopycnicity in its weak form, dashed line). Due to high depletion, high Mg#, and low  
437 compositional density, the undisturbed Archaean lithospheric mantle has lower in situ density  
438 such that isopycnicity is not satisfied.

